Structural, electronic and thermodynamic properties of magnesium chalcogenide ternary alloys

2007 J. Phys.: Condens. Matter 19 386234

(http://iopscience.iop.org/0953-8984/19/38/386234)

IOP PUBLISHING JOURNAL OF PHYSICS: CONDENSED MATTER

J. Phys.: Condens. Matter **19** (2007) 386234 (9pp) doi:10.1088/0953-8984/19/38/386234

Structural, electronic and thermodynamic properties of magnesium chalcogenide ternary alloys

F El Haj Hassan[1,3] **and B Amrani**[2]

[1] Université Libanaise, Faculté des sciences (I), Laboratoire de Physique de Matériaux, Elhadath, Beirut, Lebanon
[2] Centre Universitaire de Mascara, Mascara 29000, Algeria

E-mail: hassan.f@ul.edu.lb

Received 9 July 2007, in final form 13 August 2007
Published 4 September 2007
Online at stacks.iop.org/JPhysCM/19/386234

Abstract

The full potential–linearized augmented plane wave (FP-LAPW) method within the density functional theory (DFT) was applied to study the structural, electronic and thermodynamic properties of MgS_xSe_{1-x}, MgS_xTe_{1-x} and $MgSe_xTe_{1-x}$ ternary alloys. The calculated lattice parameters at different compositions of MgS_xSe_{1-x} and $MgSe_xTe_{1-x}$ alloys were found to vary almost linearly, while a significant deviation of the lattice parameter from Vegard's law for MgS_xTe_{1-x} alloy was observed. This is mainly due to the large mismatch of the lattice parameters of the binary compounds MgS and MgTe. A large deviation of the bulk modulus from linear concentration dependence (LCD) was observed for all three alloys. The calculated optical bowing was found to be mainly caused by the structural relaxation. Moreover, a significant charge exchange contribution was observed in the case of MgS_xTe_{1-x} alloy. The calculated phase diagram shows a broad miscibility gap for these alloys with a high critical temperature.

1. Introduction

Wide band gap II–VI semiconductors present a large interest for visible light emitters in the blue/green spectrum [1]. Compared to Mg- (belonging to column IIA in the periodic table) based semiconductors, column-IIB compounds, such as ZnSe and ZnTe, are very different in the electronic and bonding properties. This difference was attributed to the existence of a metal d band inside the main valence band in column-IIB compound semiconductors. The role of d states in II–VI semiconductors was well studied [2]. The imperfect d orbital screening in group-IIB compounds makes their atomic sizes and lattice parameters smaller than those for group-IIA compounds. The absence of a d orbital in the Mg element results in increasing the band gap [3].

[3] Author to whom any correspondence should be addressed.

Unlike ZnS, ZnSe and ZnTe, which have been extensively studied, very little is known about MgS, MgSe and MgTe. The normal structure of MgTe is wurtzite [4], while for MgS and MgSe it is zinc-blende [5], but it is possible to grow MgTe in the zinc-blende structure [6, 7].

In fact, one of the easiest ways to change artificially the electronic and optical properties of semiconductors is by forming their alloys; it is then interesting to combine two different compounds with different optical band gaps and different rigidities in order to obtain a new material with intermediate properties. Therefore, a great deal of progress has made in the last few decades in understanding the effects of disorder in random alloys. Zunger and co-workers [8] have introduced an approach that greatly reduces the size of the supercell required to obtain a realistic description of a random alloy by using so-called 'special quasirandom structures' (SQSs).

In this paper, we model MgS_xSe_{1-x}, MgS_xTe_{1-x} and $MgSe_xTe_{1-x}$ ternary alloys at some selected compositions with ordered structures described in terms of periodically repeated supercells (SQSs). In order to carry out our calculations, we have applied the full potential–linearized augmented plane wave (FP-LAPW) method. On one hand we focused our efforts on the study of the physical origins and variation of the optical band gap within the alloy fraction; on the other hand we addressed the more fundamental issue of the phase stability of these alloys.

2. Method of calculations

In order to calculate the structural and electronic properties of MgS_xSe_{1-x}, MgS_xTe_{1-x} and $MgSe_xTe_{1-x}$ alloys, we have employed the FP-LAPW method [9] to solve the Kohn–Sham equations. We have performed our calculations by the WIEN2K code [10] within the framework of density functional theory (DFT) [11], that has been shown to yield reliable results for the electronic and structural properties of various solids. The exchange–correlation contribution is described within the generalized gradient approximation (GGA) based on Perdew *et al* [12] to calculate the total energy, while for electronic properties in addition to the GGA correction the Engel–Vosko (EVGGA) [13] scheme was also applied. In the FP-LAPW approach the wavefunction, charge density and potential are expanded differently in the two regions of the unit cell. Inside the non-overlapping spheres of radius R_{MT} around each atom, spherical harmonic expansions are used, while in the remaining space of the unit cell a plane wave basis set is chosen. The muffin-tin radii R_{MT} were assumed to be 2.2 au for both Mg and S atoms, and 2.25 and 2.3 au for Se and Te atoms, respectively. A mesh of 35 special k-points for binary compounds and 27 special k-points for alloys were taken in the irreducible wedge of the Brillouin zone for the total energy calculation. The maximum l value for the wavefunction expansions inside spheres was confined to $l_{max} = 10$. The plane wave cut-off of $K_{max} = 8.0/R_{MT}$ is chosen for the expansion of the wavefunctions in the interstitial region while the charge density was Fourier expanded up to $G_{max} = 14$ (Ryd)$^{1/2}$. Both the plane wave cut-off and the number of k-points are varied to ensure total energy convergence. In order to consider the relativistic effects in our calculation, the electronic states were classified into two categories, the core and the valence states. Our calculations for valence electrons were performed in a scalar-relativistic approximation, neglecting spin–orbit coupling, while the core electrons were treated as fully relativistic.

3. Structural properties

In this section, we analyze the structural properties of MgX (X = S, Se, Te) compounds in zinc-blende structure using the GGA scheme. The alloys have been modeled at some selected

Table 1. Calculated lattice parameter (a) and bulk modulus B of MgS, MgSe and MgTe compounds and their alloys at equilibrium volume.

		Lattice constants a (Å)			Bulk modulus B (Mbar)	
	x	Our work	Exp.	Other calc.	Our work	Other calc.
MgS_xSe_{1-x}	0	6.005	5.89 [6] 5.91 [17]	5.873 [27] 5.70 [28]	45.12	47.0 [27] 64.7 [28]
	0.25	5.932			46.82	
	0.5	5.860			49.35	
	0.75	5.785			52.94	
	1	5.708	5.620 [6]	5.584 [27] 5.46 [28]	55.59	57.5 [27] 78.9 [28]
MgS_xTe_{1-x}	0	6.517	6.280 [6] 6.42 [29]		33.97	
	0.25	6.349			36.95	
	0.5	6.164			40.93	
	0.75	5.948			46.73	
	1	5.708	5.620 [6]	5.584 [27] 5.46 [28]	55.59	57.5 [27] 78.9 [28]
$MgSe_xTe_{1-x}$	0	6.517	6.280 [6] 6.42 [29]		33.97	
	0.25	6.407			36.02	
	0.5	6.283			38.43	
	0.75	6.148			41.21	
	1	6.005	5.89 [6] 5.91 [17]	5.873 [27] 5.70 [28]	45.12	47.0 [27] 64.7 [28]

compositions ($x = 0.25, 0.5, 0.75$) following the SQS approach. For the considered structures, we perform the structural optimization by minimizing the total energy with respect to the cell parameters and also the atomic positions.

The total energies calculated as a function of unit cell volume were fitted to the Murnaghan's equation of state [14]. The corresponding equilibrium lattice constants and bulk modulus both for binary compounds and their alloys are given in table 1. Considering the general trend that GGA usually overestimates the lattice parameters [15], our GGA results of binary compounds are in reasonable agreement with the experimental and other calculated values.

Usually, in the treatment of alloys, it is assumed that the atoms are located at the ideal lattice sites and the lattice constant varies linearly with composition x according to the so-called Vegard's law [16]. However, violation of this linear law has been reported in semiconductor alloys both experimentally [17, 18] and theoretically [19, 20]. Our calculated lattice parameters at different compositions of MgS_xSe_{1-x} and $MgSe_xTe_{1-x}$ alloys were found to vary almost linearly with a marginal upward bowing parameter equal to -0.01 and -0.08 Å, respectively, while the variation of the calculated equilibrium lattice constant versus concentration for MgS_xTe_{1-x} alloy exhibits a significant deviation from Vegard's law with upward bowing parameters equal to -0.20 Å. The physical origin of this deviation should be mainly due to the large mismatches of the lattice constants of MgS and MgTe compounds.

A deviation of the bulk modulus from the linear concentration dependence (LCD) with downward bowing equal to 3.37, 15.52 and 4.67 GPa for MgS_xSe_{1-x}, MgS_xTe_{1-x} and $MgSe_xTe_{1-x}$ alloys, respectively, was observed. The large value of the bulk modulus bowing for MgS_xTe_{1-x} alloy compared to the two other corresponding alloy values originates in the significant mismatch of the bulk modulus of MgS and MgTe compounds.

The charge density is an appropriate tool that provides us with a better understand of the bonding character in these compounds, and FP-LAPW gives an accurate description of the valence charge density. We then correlate this latter quantity to the ionicity factor through an empirical formula [21], which has been successfully applied to other A^NB^{8-N} compounds [22].

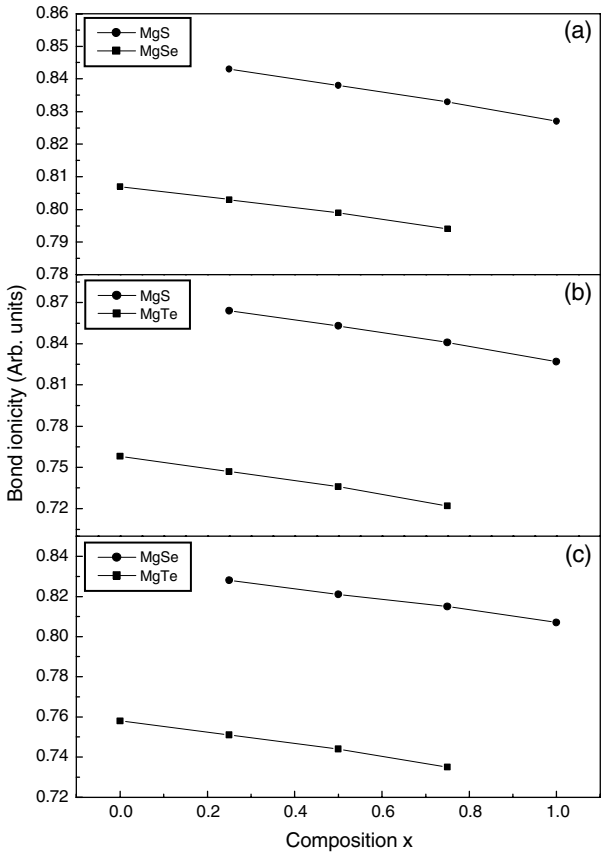

Figure 1. The ionicity variation of the calculated bonds versus concentration for (a) MgS_xSe_{1-x}, (b) MgS_xTe_{1-x} and (c) $MgSe_xTe_{1-x}$ alloys.

In figure 1, we show the ionicity of the bonds at different concentrations. It is relevant to note that for all three alloys the ionicity increases linearly on going from $x = 0$ to 1 with slopes equal to 0.017, 0.049 and 0.028 for MgS_xSe_{1-x}, MgS_xTe_{1-x} and $MgSe_xTe_{1-x}$ alloys, respectively. Our results indicate that the slope values have a significant effect on the charge-exchange contribution to the optical bowing as shown in the next section.

4. Optical bowing and its origins

The self consistent scalar relativistic band gap of MgX compounds and their alloys was calculated within the GGA and EVGGA schemes. A direct band gap has been observed for all the materials under investigation and the results are presented in table 2. The GGA functionals have simple forms that are not sufficiently flexible to accurately reproduce both exchange–correlation energy and its charge derivative. Engel and Vosko on considering this shortcoming constructed a new functional form of GGA which is able to better reproduce exchange potential at the expense of less agreement in exchange energy. This approach, which is called EVGGA, yields a better band splitting and some other properties, which mainly depend on the accuracy of the exchange–correlation potential. On the other hand, in this method, the quantities which

Table 2. Direct band gap energy of zinc chalcogenide compounds and their alloys at equilibrium volume (all values are in eV).

		Eg (eV)			
		Our work			
	x	GGA	EVGGA	Exp.	Other calc.
MgS_xSe_{1-x}	0	2.494	3.529	3.59 [6] 4.05 [7]	2.8 [27] 3.3 [28]
	0.25	2.712	3.809		
	0.5	2.909	4.030		
	0.75	3.122	4.272		
	1	3.333	4.418	4.45 [6]	3.42 [27] 3.7 [28]
MgS_xTe_{1-x}	0	2.293	3.153	3.49 [7]	
	0.25	2.407	3.335		
	0.5	2.609	3.607		
	0.75	2.939	4.008		
	1	3.333	4.418	4.45 [6]	3.42 [27] 3.7 [28]
$MgSe_xTe_{1-x}$	0	2.293	3.153	3.49 [7]	
	0.25	2.300	3.199		
	0.5	2.334	3.277		
	0.75	2.398	3.386		
	1	2.494	3.529	3.59 [6] 4.05 [7]	2.8 [27] 3.3 [28]

Table 3. Decomposition of the optical bowing into volume deformation (VD), charge exchange (CE) and structural relaxation (SR) contributions compared with that obtained by a quadratic fit and other predictions (all values are in eV).

		Present work				
		Zunger approach		Quadratic eq.		
		GGA	EVGGA	GGA	EVGGA	Other calc.
MgS_xSe_{1-x}	b_{VD}	0.033	0.057			
	b_{CE}	−0.042	−0.040			
	b_{SR}	0.026	0.036			
	b	0.017	0.053	0.013	0.060	0.12 [25] 0.49 [30]
MgS_xTe_{1-x}	b_{VD}	−0.019	−0.054			
	b_{CE}	0.373	0.305			
	b_{SR}	0.422	0.462			
	b	0.776	0.713	0.786	0.678	
$MgSe_xTe_{1-x}$	b_{VD}	−0.009	−0.010			
	b_{CE}	0.083	0.020			
	b_{SR}	0.162	0.217			
	b	0.236	0.227	0.238	0.257	

depend on an accurate description of exchange energy E_x such as equilibrium volumes and bulk modulus are far from experiment. Therefore we always apply EVGGA to the electronic properties and GGA for the structural properties [23, 24].

The composition dependence of the calculated band gaps using GGA and EVGGA schemes was found to vary non-linearly, producing gap bowing. The results, obtained by quadratic fit, are presented and compared with the other available predictions in table 3. These

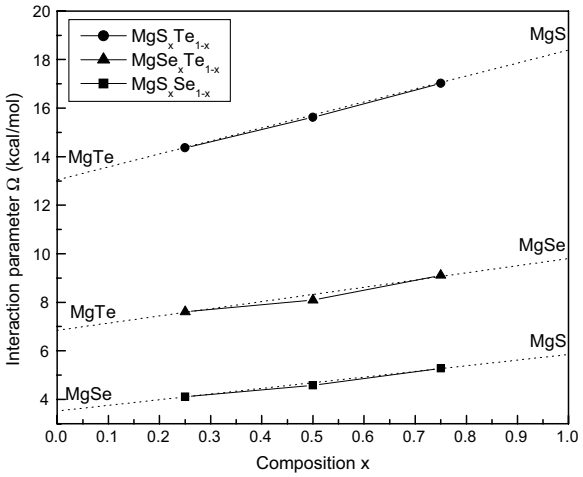

Figure 2. Interaction parameter, Ω, as a function of the composition x calculated for MgS_xSe_{1-x} (solid squares), MgS_xTe_{1-x} (solid circles) and $MgSe_xTe_{1-x}$ (solid triangles) alloys. The dashed lines are the linear fit to the Ω values.

results obey the following variations:

$$MgS_xSe_{1-x} \Rightarrow \begin{cases} E_g^{GGA}(x) = 2.497 + 0.832x + 0.013x^2, \\ E_g^{EVGGA}(x) = 3.589 + 0.861x + 0.060x^2. \end{cases} \quad (1)$$

$$MgS_xTe_{1-x} \Rightarrow \begin{cases} E_g^{GGA}(x) = 2.292 + 0.258x + 0.786x^2, \\ E_g^{EVGGA}(x) = 3.148 + 0.600x + 0.678x^2. \end{cases} \quad (2)$$

$$MgSe_xTe_{1-x} \Rightarrow \begin{cases} E_g^{GGA}(x) = 2.293 - 0.038x + 0.238x^2, \\ E_g^{EVGGA}(x) = 3.153 + 0.118x + 0.257x^2. \end{cases} \quad (3)$$

It is noticeable that our EVGGA calculated optical bowing value for MgS_xSe_{1-x} alloy is in good agreement with that calculated using the empirical pseudopotential method [25].

The physical origins of gap bowing were investigated following the approach of Zunger and co-workers [26], which decomposes it into three contributions:

$$b = b_{VD} + b_{CE} + b_{SR}. \quad (4)$$

The corresponding contribution to the total gap bowing parameter b_{VD} represents the relative response of the band structure of the binary compounds AB and AC to hydrostatic pressure, which here arises from the change of their individual equilibrium lattice constants to the alloy value $a = a(x)$ (from Vegard's rule). The second contribution, the charge-exchange (CE) contribution b_{CE}, reflects a charge transfer effect which is due to the different (averaged) bonding behavior at the lattice constant a. The final step measures changes due to the structural relaxation (SR) in passing from the unrelaxed to the relaxed alloy by b_{SR}.

The calculated gap bowing contributions of the direct band gap are presented in table 3. It is clearly seen that the calculated quadratic parameters (gap bowing) within GGA and EVGGA are very close to the results obtained by the Zunger approach. The optical bowing of MgS_xSe_{1-x} alloy was found to be small compared with the two other alloys. The total gap bowing of MgS_xTe_{1-x} and $MgSe_xTe_{1-x}$ alloys was mainly caused by the structural relaxation b_{SR}. The charge transfer contribution b_{CE} has been found to be more significant in MgS_xTe_{1-x}

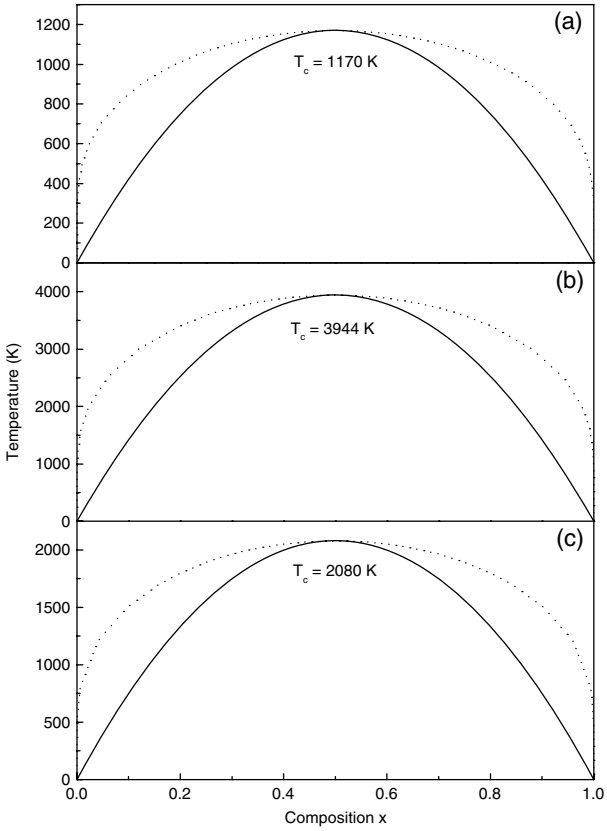

Figure 3. T–x phase diagram of (a) MgS_xSe_{1-x}, (b) MgS_xTe_{1-x} and (c) $MgSe_xTe_{1-x}$ alloys. Dashed line: binodal curve. Solid line: spinodal curve.

alloy than the two other alloys; this is correlated to the ionicity factor difference among constituent binary compounds as shown at the end of section 3.

5. Thermodynamic properties

Herein we present a rigorous theoretical study of the thermodynamic properties of MgS_xSe_{1-x}, MgS_xTe_{1-x} and $MgSe_xTe_{1-x}$ alloys; the calculations carried out here are based on the *ab initio* method. We calculate the Gibbs free energy of mixing $\Delta G_m(x, T)$, which allows us to access the T–x phase diagram and obtain the critical temperature, T_c, for miscibility. Details of the calculations are given in [19]. Indeed, an important contribution arises from the mixing enthalpy, which can be obtained from the calculated total energies. We then calculated the interaction parameter (Ω) as a function of concentration. Figure 2 shows Ω versus x for MgS_xSe_{1-x}, MgS_xTe_{1-x} and $MgSe_xTe_{1-x}$ alloys. From a linear fit we obtained

$$MgS_xSe_{1-x} \Rightarrow \Omega(\text{kcal mol}^{-1}) = 3.49 + 2.33x, \tag{5}$$

$$MgS_xTe_{1-x} \Rightarrow \Omega(\text{kcal mol}^{-1}) = 13.02 + 5.30x, \tag{6}$$

$$MgSe_xTe_{1-x} \Rightarrow \Omega(\text{kcal mol}^{-1}) = 6.77 + 3.00x. \tag{7}$$

The average values of the x-dependent Ω in the range $0 \leqslant x \leqslant 1$ obtained from these equations for MgS_xSe_{1-x}, MgS_xTe_{1-x} and $MgSe_xTe_{1-x}$ alloys are 4.65, 15.67 and 8.27 (kcal mol^{-1})

respectively. The larger enthalpy for MgS_xTe_{1-x} alloy suggests a large value of Ω and hence a higher critical temperature.

We calculated the temperature–composition phase diagram which shows the stable, metastable and unstable mixing regions of the alloy. At a temperature lower than the critical temperature T_c, the two binodal points are determined as those points at which the common tangent line touches the ΔG_m curves. The two spinodal points are determined as those points at which the second derivative of ΔG_m is zero.

Figure 3 displays the calculated phase diagrams including the spinodal and binodal curves of the alloys of interest. We observed a critical temperature T_c of 1170, 3944 and 2080 K for MgS_xSe_{1-x}, MgS_xTe_{1-x} and $MgSe_xTe_{1-x}$ alloys, respectively. The spinodal curve in the phase diagram marks the equilibrium solubility limit, i.e. the miscibility gap. For temperatures and compositions above this curve a homogeneous alloy is predicted. The wide range between spinodal and binodal curves indicates that the alloy may exist as metastable phase.

6. Conclusions

In summary, we have studied the structural, electronic and thermodynamic properties of MgS_xSe_{1-x}, MgS_xTe_{1-x} and $MgSe_xTe_{1-x}$ alloys by using the FP-LAPW method. Deviation of the lattice constant from Vegard's law was observed for MgS_xTe_{1-x} alloy, while the calculated lattice parameters at different compositions for MgS_xSe_{1-x} and $MgSe_xTe_{1-x}$ alloys were found to vary almost linearly. This is mainly due to the large mismatch of the lattice parameters of the binary compounds MgS and MgTe. A nonlinear dependence on the composition x was observed for the bulk modulus of all three alloys. The gap bowing is found to be significant for MgS_xTe_{1-x} alloy and mainly cased by the structural relaxation effect. The charge exchange contribution, although smaller than the first contribution, is not ignorable. The investigation of the thermodynamic stability allowed us to calculate the critical temperatures for MgS_xSe_{1-x}, MgS_xTe_{1-x} and $MgSe_xTe_{1-x}$ alloys, which are 1170, 3944 and 2080, respectively.

References

[1] Gunshor R L and Nurmikko A V (ed) 1997 II–VI blue/green light emitters: devices physics and epitaxial growth *Semiconductor and Semimetals* vol 44 (New York: Academic)

[2] Wei S-H and Zunger A 1988 *Phys. Rev.* B **37** 8958

[3] Chadi D J 1994 *Phys. Rev. Lett.* **72** 534

[4] Parker S G, Reinberg A R, Pinnell J E and Holton W C 1971 *J. Electrochem. Soc.* **118** 979

[5] Broser I, Broser R, Finkenrath H, Galazka R R, Gumlich H E, Hoffmann A, Kossut J, Mollwo E, Nelkowski H, Nimtz G, Osten W, Rosenzweig M, Schulz H J, Theis D and Tschierse D 1982 *Physics of II–VI and I–VII Compounds, Semimagnetic Semicondectors* vol 17 b ed O Madelung and Landolt-Börnstein (Berlin: Springer) p 10

[6] Okuyama H, Kishita Y and Ishibashi A 1998 *Phys. Rev.* B **57** 2257

[7] Litz M T, Watanabe K, Korn M, Ress H, Lunz U, Ossau W, Waag A, Landwehr G, Walter T, Neubauer B, Gerthsen D and Schüssler U 1996 *J. Cryst. Growth* **159** 54

[8] Zunger A, Wei S-H, Ferreira L G and Bernard E 1990 *Phys. Rev. Lett.* **65** 353
Wei S-H, Ferreira L G, Bernard J E and Zunger A 1990 *Phys. Rev.* B **42** 9622

[9] Koelling D D and Harmon B N 1977 *J. Phys. C: Solid State Phys.* **10** 3107

[10] Blaha P, Schwarz K, Madsen G K H, Kvasnicka D and Luitz J 2001 *WIEN2K, An Augmented Plane Wave +Local Orbitals Program for Calculating Crystal Properties* Karlheinz Schwarz, Techn. Universitat, Wien, Austria (ISBN 3-9501031-1-2)

[11] Kohn W and Sham L J 1965 *Phys. Rev.* A **140** 1133
Hohenberg P and Kohn W 1964 *Phys. Rev.* B **136** 864

[12] Perdew J P, Burke S and Ernzerhof M 1996 *Phys. Rev. Lett.* **77** 3865

[13] Engel E and Vosko S H 1993 *Phys. Rev.* B **47** 13164

[14] Murnaghan F D 1944 *Proc. Natl Acad. Sci. USA* **30** 244
[15] Charifi Z, Baaziz H, El Haj Hassan F and Bouarissa N 2005 *J. Phys.: Condens. Matter* **17** 4083
[16] Vegard L 1921 *Z. Phys.* **5** 17
[17] Jobst B, Hommel D, Lunz U, Gerhard T and Landwehr G 1996 *Appl. Phys. Lett.* **69** 97
[18] Dismuckes J P, Ekstrom L and Poff R J 1964 *J. Phys. Chem.* **68** 3021
[19] El Haj Hassan F and Akdarzadeh H 2005 *Mater. Sci. Eng.* B **121** 170
[20] El Haj Hassan F 2005 *Phys. Status Solidi* b **242** 909
[21] Zaoui A, Ferhat M, Khelifa B, Dufour J P and Aourag H 1994 *Phys. Status Solidi* b **185** 163
[22] El Haj Hassan F, Zaoui A and Sekkal W 2001 *Mater. Sci. Eng.* B **87** 40
El Haj Hassan F, Akbarzadeh H and Zoaeter M 2004 *J. Phys.: Condens. Matter* **16** 293
[23] Dufek P, Blaha P and Schwarz K 1994 *Phys. Rev.* B **50** 7279
[24] El Haj Hassan F, Akbarzadeh H and Hashemifar S J 2004 *J. Phys.: Condens. Matter* **16** 3329
El Haj Hassan F, Akdarzadeh H, Hashemifar S J and Mokhatari A 2004 *J. Phys. Chem. Solids* **65** 1871
[25] Charifi Z, Baaziz H and Bouarissa N 2003 *Physica* B **337** 363
[26] Bernard J E and Zunger A 1986 *Phys. Rev. Lett.* **34** 5992
Wei S-H, Ferreira L G, Bernard J E and Zunger A 1990 *Phys. Rev.* B **42** 9622
[27] Lee S G and Chang K J 1995 *Phys. Rev.* B **52** 1918
[28] Kalpana G, Palanivel B, Thomas R M and Rajagopalan M 1996 *Physica* B **222** 223
[29] Watanabe K, Litz M T, Korn M, Ossau W, Waag A, Landwehr G and Schüssler U 1997 *J. Appl. Phys.* **81** 451
[30] Rabah M, Abbar B, Al-Douri Y, Bouhafs B and Sahraoui B 2003 *Mater. Sci. Eng.* B **100** 163